

## Detection of urea-induced internal denaturation of dsDNA using solid-state nanopores

This article has been downloaded from IOPscience. Please scroll down to see the full text article.

2010 J. Phys.: Condens. Matter 22 454111

(<http://iopscience.iop.org/0953-8984/22/45/454111>)

View [the table of contents for this issue](#), or go to the [journal homepage](#) for more

Download details:

IP Address: 128.197.58.60

The article was downloaded on 30/06/2011 at 23:48

Please note that [terms and conditions apply](#).

# Detection of urea-induced internal denaturation of dsDNA using solid-state nanopores

Alon Singer, Heiko Kuhn, Maxim Frank-Kamenetskii and Amit Meller<sup>1</sup>

Department of Biomedical Engineering, Boston University, Boston, MA 02215, USA

E-mail: [ameller@bu.edu](mailto:ameller@bu.edu)


Received 5 April 2010, in final form 6 May 2010

Published 29 October 2010

Online at [stacks.iop.org/JPhysCM/22/454111](http://stacks.iop.org/JPhysCM/22/454111)

## Abstract

The ability to detect and measure dsDNA thermal fluctuations is of immense importance in understanding the underlying mechanisms responsible for transcription and replication regulation. We describe here the ability of solid-state nanopores to detect sub-nanometer changes in DNA structure as a result of chemically enhanced thermal fluctuations. In this study, we investigate the subtle changes in the mean effective diameter of a dsDNA molecule with 3–5 nm solid-state nanopores as a function of urea concentration and the DNA's AT content. Our studies reveal an increase in the mean effective diameter of a DNA molecule of approximately 0.6 nm at 8.7 M urea. In agreement with the mechanism of DNA local denaturation, we observe a sigmoid dependence of these effects on urea concentration. We find that the translocation times in urea are markedly slower than would be expected if the dynamics were governed primarily by viscous effects. Furthermore, we find that the sensitivity of the nanopore is sufficient to statistically differentiate between DNA molecules of nearly identical lengths differing only in sequence and AT content when placed in 3.5 M urea. Our results demonstrate that nanopores can detect subtle structural changes and are thus a valuable tool for detecting differences in biomolecules' environment.

 Online supplementary data available from [stacks.iop.org/JPhysCM/22/454111/mmedia](http://stacks.iop.org/JPhysCM/22/454111/mmedia)

(Some figures in this article are in colour only in the electronic version)

## 1. Introduction

Solid-state nanopores have emerged as one of the most effective tools for probing unmodified biopolymers at the single-molecule level [1–5]. The concept of resistance-based measurements to probe particles passing through an orifice is not a new one as it was first described by Coulter in the late 1940s [6, 7]. Nanopores however, take this method to the next level, by using nanoscale apertures to linearize and characterize molecules rather than cells or micron-sized particles. Typically, in the solid-state nanopore method, a small nanoscale aperture is created or fabricated through the use of a high-intensity electron or ion beam irradiated onto an ultra-thin insulating membrane of SiN, SiO<sub>2</sub>, or Al<sub>2</sub>O<sub>3</sub> embedded on

a Si support chip [8–11]. After fabrication, the nanopore chip is immersed between two chambers filled with an electrolyte solution, thus hydrating the nanopore. Voltage is then applied across this ultra-thin membrane, creating a measurable ion-based current. Upon addition of charged biopolymers (e.g. nucleic acids or proteins), the space-dependent electrical field funnels these macromolecules, which randomly approach the pore vicinity by diffusion, towards and then across the nanopore [12]. This passage or translocation of the biopolymer across the nanopore results in a transient increase in the resistance of the nanopore and, accordingly, causes a reduction in the measured current. Upon completion of the translocation process, the current returns to its previous level. Solid-state nanopores are considered highly advantageous, as they allow a high-throughput and purely electrical probing of individual biopolymers without the need for time-consuming and/or

<sup>1</sup> Author to whom any correspondence should be addressed.

complex sample preparation. Thus, solid-state nanopores offer numerous potential advantages for the development of improved methods for DNA sequencing, genotyping, and high-throughput screening [13–17].

Recent advances in nanoscale fabrication techniques allow the construction of nanoscale devices with unprecedented control of properties such as composition, location, and dimension. Therefore, with the ability to fabricate nanopores with sub-nanometer resolution in the 3–5 nm range, it has become possible not only to probe biopolymers, but to *unfold* and *linearize* them as they are forced to pass through the nanopore [18]. As such, it has recently been demonstrated that solid-state nanopores in this size range have the ability to be sensitive to different DNA lengths, intercalating molecules, and synthetic binding probes. It is this linearization process which gives nanopores their inherent sensitivity to DNA size and structure [15, 17, 18].

With pores significantly larger than the hydrodynamic diameter of DNA, it has been established that it is possible to differentiate between folded and unfolded translocation events, simply by observing the blockade events; unfolded events inherently induce a smaller restriction than those of folded translocation events [19]. By constricting the nanopore to a diameter only slightly larger than the biopolymer's hydrodynamic diameter, it has been shown that it is possible to differentiate between the native DNA structure and structures that are altered due to ligand binding [15, 17]. Further constriction of the nanopore to diameters below 2 nm, which are smaller than the hydrodynamic diameter of double-stranded DNA (dsDNA), allows the unzipping of DNA hairpins as previously described by McNally *et al* [20]. Small pore dimensions are additionally advantageous because they increase the passage dwell-time of the biomolecules, thus improving the temporal resolution of the method. With these advantages, the 3–5 nm pores offer optimal resolution for monitoring changes in DNA structure.

In this study we set out to investigate the ability of solid-state nanopores to detect small variances in dsDNA cross-section due to the presence of denaturants. It is well known that different conformational transitions can be induced in the typical B-form DNA by changes in temperature and the addition of cosolutes [21]. Among those transitions, the DNA melting transition has been perhaps the most thoroughly studied. It has been well established that, even at temperatures well below the melting range, fluctuating openings of the DNA double helix occur. These openings make the bases, normally buried within the double helix, accessible to hydrogen exchange and reactions with chemicals, such as formaldehyde, and to interactions with proteins, such as RNA polymerase [22–24]. Due to the potentially important functional roles of these thermal fluctuations, a number of theoretical and experimental approaches are being employed and developed to study these processes in order to gain insights into their underlying dynamics and geometry as well as likelihood of formation. Herein, we demonstrate for the first time that solid-state nanopores, through the powerful attribute of linearizing dsDNA, have the ability to probe for these thermal fluctuations.

## 2. Materials and methods

Nanopores were fabricated in-house in a 30 nm thick, low-stress LPCVD Si<sub>3</sub>N<sub>4</sub> film (SiN) in which a 10  $\mu\text{m} \times 10 \mu\text{m}$  window was exposed through KOH wet etching. Pores were fabricated in the SiN film using a highly focused electron beam, as previously described [10]. Chips were cleaned with a piranha solution and assembled on a custom-designed cell under a controlled atmosphere [4]. Nanopores were hydrated with the addition of degassed and filtered (0.02  $\mu\text{m}$ ) KCl electrolyte solution buffered with 10 mM Tris-HCl to pH 8.5. Electrolyte strength was typically 1 M/1 M KCl *cis/trans* or 0.2 M/2 M KCl *cis/trans* in the 150 bp translocation studies. Asymmetric salt concentrations across the membrane significantly increase the dwell-time, while having little effect on the normalized blockade level, thus permitting detection of relatively short DNAs [12]. In experiments where urea was used, urea was added to the desired weight/weight concentration, maintaining electrolyte strength and pH values. Ag/AgCl electrodes were immersed into each chamber of the cell and connected to an Axon 200B headstage. All measurements were made inside a dark Faraday cage. All measurements were performed using a 50 kHz low-pass Butterworth filter, and sampled using a 16-bit/250 kHz DAQ card, operated with our custom LabView software. In all cases, DNA was added to the *cis* chamber, where, upon the application of the 300 mV positive bias to the *trans* chamber, the DNA migrated linearly through the pore from the *cis* to the *trans* side (figure 1(A)). All studies were conducted using nanopores in the 3–5 nm diameter range as indicated (figure 1(B)). We define the following parameters for each DNA translocation event (see figure 1(C)): (1)  $i_o$  denotes the *mean* open pore current at the applied voltage bias, measured just prior or after the event; (2)  $i_b$  represents the mean blocked ion current level during DNA transport through the pore; (3)  $I_B = i_b/i_o$  is the fractional blocked current; and (4)  $t_D$  represents the dwell-time of a DNA molecule in the pore. In this study, we exclude short (<25  $\mu\text{s}$ ) intermittent current blockades due to DNA collisions rather than full translocation, as described by Wanunu *et al* [18].

### 2.1. Sample preparation

The 800 bp long DNA fragment (45% AT content) was purchased from Fermentas (NoLimits™ DNA fragment, Burlington, Ontario, Canada). Oligonucleotides were purchased from Integrated DNA Technologies (Coralville, IA). DNA concentrations were determined on a NanoDrop ND-1000 spectrophotometer. Taq DNA polymerase and DyNAzyme EXT DNA polymerase were obtained from New England BioLabs (Ipswich, MA). *Escherichia coli* K-12 MG1655 strain was obtained from ATCC (Manassas, VA). *E. coli* culture was grown in Luria Bertani broth for 16 h at 37 °C, and genomic DNA was isolated using the Qiagen DNeasy Blood and Tissue Kit.

### 2.2. PCR

For amplification of fragments D807, AT<sub>80</sub>, AT<sub>68</sub>, and AT<sub>49</sub>, reactions were performed in 1  $\times$  Thermo Pol buffer containing

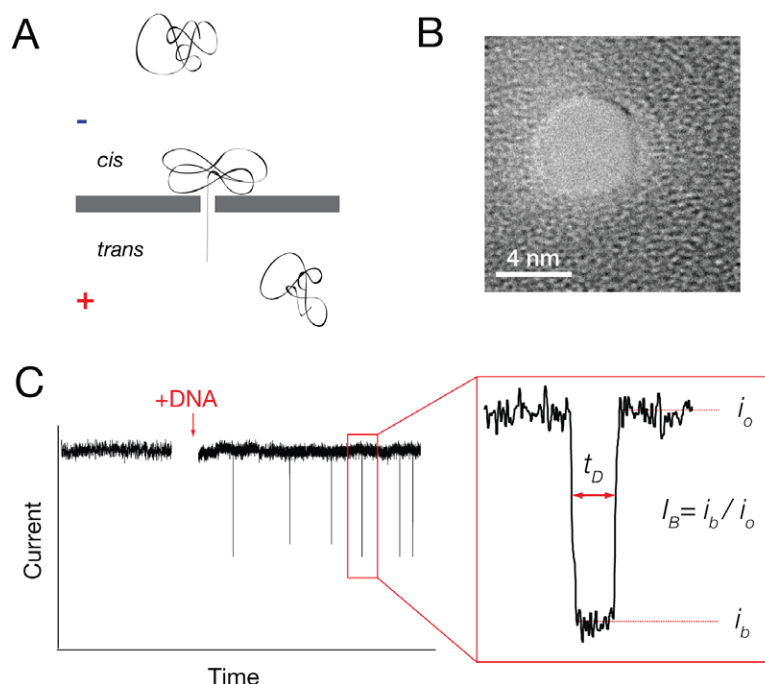


**Figure 1.** Studying individual DNA molecules using solid-state nanopores. (A) A schematic diagram depicting the unfolding/linearization process which a DNA molecule undergoes as it translocates across a 3–5 nm pore from the *cis* to the *trans* side of an ultra-thin membrane. (B) A high-resolution TEM image of a 4 nm pore (scale bar represents 4 nm). (C) Prior to the addition of DNA molecules to the *cis* chamber, a constant current is measured. With the addition of DNA molecules to the *cis* chamber, transient downward spikes become apparent, indicating the passage or translocation of a single DNA molecule across the pore. Through a close-up view of an individual event one can determine the dwell-time,  $t_D$ , and the blockade level,  $i_b$ . The relative blockade level,  $I_B$ , is calculated by the ratio of  $i_b/i_o$ , where  $i_o$  is the mean current before and after a translocation event.

0.1 ng  $\mu\text{l}^{-1}$  *E. coli* genomic DNA, 400  $\mu\text{M}$  of each dNTP, 0.5  $\mu\text{M}$  each of a corresponding primer pair, and 0.02 units  $\mu\text{l}^{-1}$  of Taq DNA polymerase. For amplification of fragment AT<sub>28</sub>, reactions were carried out in 1× DyNAzyme buffer containing 5% DMSO and 0.03 units  $\mu\text{l}^{-1}$  of DyNAzyme EXT DNA polymerase. Amplification was carried out with an initial denaturation step at 93 °C for 180 s, followed by 30 cycles of denaturation, primer annealing, and extension. Durations and temperatures of the steps within a cycle differed for the amplification of each fragment and can be found in the supporting information (available at [stacks.iop.org/JPhysCM/22/454111/mmedia](http://stacks.iop.org/JPhysCM/22/454111/mmedia)). All PCR amplicons were purified by QIAquick PCR purification kit (Qiagen) and analyzed on 1% agarose gels.

### 3. Results

In figure 2(A) we present typical current–voltage ( $I$ – $V$ ) curves measured using a 4.3 nm pore immersed in either water buffer (solid blue symbols) or in concentrated urea buffer (45% w/w or  $\sim 8.7$  M urea, open red symbols). Two prominent features are readily apparent. First, in both cases the  $I$ – $V$  curves are linear and symmetrical, indicating a symmetrical pore structure and the lack of preferential interactions between the urea and the migrating ions. Second, we note that the reduction in pore conductance can be fully explained by the increased bulk viscosity of the 45% urea solution (1.8 cP). Moreover, we find that repeated measurements with the same solid-state nanopore in buffers with different concentrations

of urea result in an extremely reproducible *relative* change in pore conductivity, which is independent of the exact pore diameter and perfectly matches the change in solution viscosity. This result is illustrated in figure 2(B), where the ratio of water/urea conductivity,  $G_W/G_U$ , (solid red symbols) and the solution viscosity  $\eta$  (open symbols) are plotted against the urea concentration (from 0% to 45% w/w). Experiments using different pore sizes yielded the same behavior (data not shown). These results are readily explainable given that, to a first approximation, the nanopore conductivity is proportional to the product of ion mobility and the form factor of the nanopore [10]. Note that the latter remains fixed as we switch from water buffer to urea buffer. The ionic electrophoretic mobility can be approximated by a factor proportional to  $1/\eta$ , where  $\eta$  is the dynamic viscosity of the system, as well as the ions' concentration, which is kept constant in these experiments [25].

Next we examined the ability of the solid-state nanopores to discriminate between dsDNA molecules having the same length ( $\sim 150$  bp) but different AT (adenine–thymine base pairs) contents. Thermal fluctuations in AT-rich regions can give rise to local points of DNA denaturation, in which the two strands are separated by about 0.2 nm, even well below their global melting temperatures. We hypothesized that in our typical, non-urea and high salt buffer, the distributions of the fractional pore current ( $I_B$ ) would be insensitive to AT-content variation due to the low probability of local denaturation of DNA. However, with the addition of  $\sim 3.5$  M urea (20% w/w) to the system (a well established nucleic acid denaturant [26]),

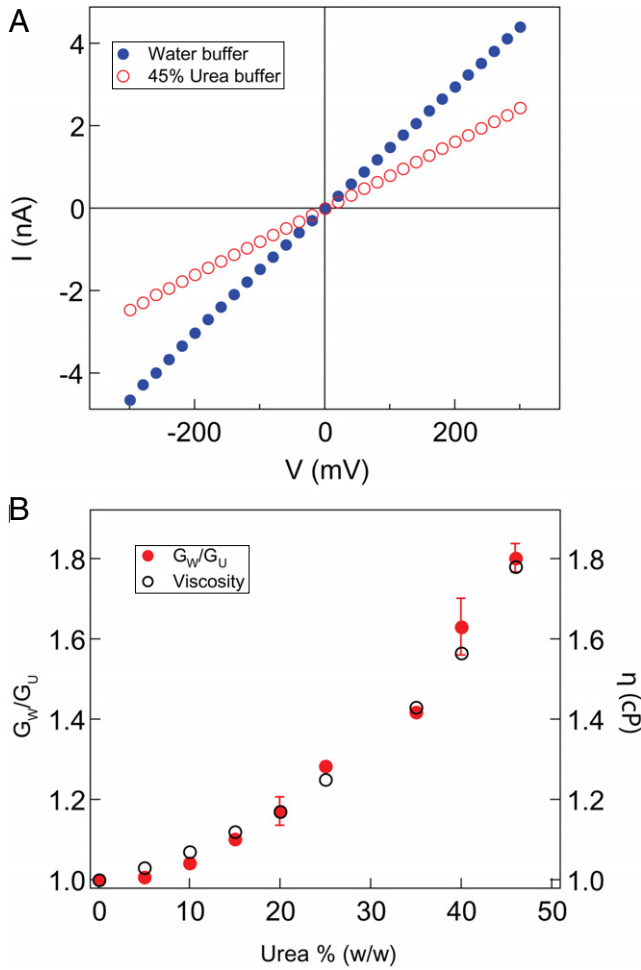


**Figure 2.** (A)  $I$ - $V$  measurements using a 4.3 nm pore immersed in either non-urea (water) or 45% urea buffer (solid blue or open red symbols, respectively), showing linear and symmetrical behavior. (B) The dependence of pore conductivity on urea concentration, normalized to the conductivity of the same pore in non-urea buffer (solid red circles). The solution viscosity is overlaid in open circles (right axis).

enhanced local DNA denaturation is expected to occur, and a shift in the mean value of  $I_B$  should be observed as a function of the AT content. To test this hypothesis we amplified different regions of the *E. coli* genome, which contained the desired AT content, by polymerase chain reaction (PCR). Four different DNA fragments of nearly identical length ( $\sim 150$  bp; sequences, PCR conditions, and analysis of amplicons are given in the supporting information and figure SI-1 available at [stacks.iop.org/JPhysCM/22/454111/mmedia](http://stacks.iop.org/JPhysCM/22/454111/mmedia)) were prepared with the following AT contents: AT<sub>28</sub> (27.7%), AT<sub>49</sub> (48.6%), AT<sub>68</sub> (68.0%), and AT<sub>80</sub> (80.0%).

Translocation measurements of short DNA strands (i.e. 150 bp) using solid-state pores larger than 5 nm are challenging since the residence time of the DNA molecules in the pores approaches the system's effective bandwidth [18]. Here we take advantage of two recent findings to facilitate accurate measurements of the blocked ion current (and hence  $I_B$ ) and translocation time of relatively short DNA molecules: first, an exponential increase in the characteristic translocation time is obtained with decreasing the pore diameter below

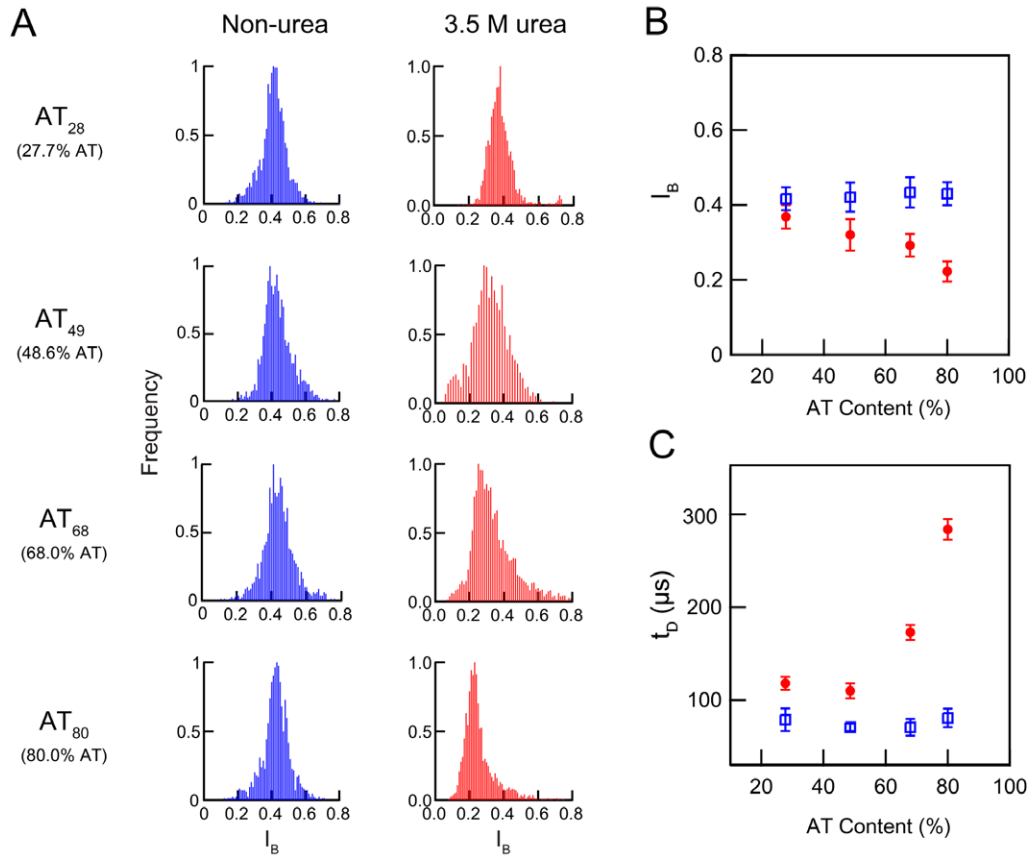
5 nm [18]. Thus, reducing the pore size from  $\sim 5$  to 3 nm results in an increase of translocation duration of more than an order of magnitude. Second, an additional linear increase in translocation time can be achieved by employing a salt gradient in the two chambers [12]. Here we use 3.0 nm solid-state pores and a salt gradient ( $[KCl]_{trans}/[KCl]_{cis} \sim 10$ ), which when combined lead to a characteristic translocation time of 75  $\mu s$  under 300 mV and at room temperature: easily measurable with our 50 kHz bandwidth.

Figure 3(A) displays the  $I_B$  distributions measured for the four different DNA fragments in a non-urea buffer (left column, blue) or a 3.5 M urea buffer (right column, red). In each case at least 2000 translocation events were acquired in order to obtain statistically reliable results. Our data indicate that, under non-urea conditions, the  $I_B$  values for all of the molecules remain similar ( $I_B = 0.42 \pm 0.05$ ), as expected. By contrast, under urea conditions we identify a systematic reduction in the most probable  $I_B$  value (from 0.38 to 0.25) as the AT content of DNA sample increases. In figure 3(B), we display the dependence of the most probable  $I_B$  values on the AT content in the absence and presence of urea (same color code as in figure 3(A)). Clearly, in the presence of urea, a higher AT content is expected to result in a larger sum of domains with local DNA denaturation; evidently such domains are readily detectable with solid-state nanopores. Additionally, we note that the characteristic dwell-times ( $t_D$ ) of the translocation events measured in these experiments exhibit a consistent trend: while the  $t_D$  values remain insensitive to the AT content in the non-urea buffer, a marked increase in  $t_D$  is observed with increasing AT content of samples when experiments are performed in 3.5 M urea. In summary, under partial denaturing conditions (3.5 M urea), as the AT content increases, DNA molecules require a longer amount of time to translocate across the pore and induce a smaller fractional blocked current level. Since all experiments were performed under identical conditions with or without urea, the differences in blockade levels and translocation times can be clearly attributed to differences in DNA structure induced by the presence of this denaturant. Furthermore, we validate the urea-induced structural alterations by performing bulk circular dichroism (CD) measurements (see figure SI-3 available at [stacks.iop.org/JPhysCM/22/454111/mmedia](http://stacks.iop.org/JPhysCM/22/454111/mmedia)). Notably, CD studies have been used in the past to characterize structural changes in dsDNA in the presence of denaturants [27, 28]. Our bulk results are consistent with the formation of local denaturation of dsDNA.

In order to better understand the sensitivity of the nanopore signals to small, urea-induced thermal fluctuations, we performed an extensive DNA translocation study by gradually changing the urea concentration from 0% to 45% w/w in small increments. Our previous studies indicated that the average fractional blocked current  $I_B$  can be accurately estimated by the ratio of the mean diameter of the molecule to the pore diameter, namely [18]

$$\bar{I}_B = 1 - \left( \frac{\bar{a}}{d} \right)^2, \quad (1)$$





**Figure 3.** Translocation studies of  $\sim 150$  bp DNA samples differing in AT content in 3.5 M urea. (A)  $I_B$  distributions measured using the same  $\sim 3$  nm solid-state pore ( $N > 2000$  events) immersed in either non-urea (left column, blue) or 3.5 M urea (right column, red) buffers. The different AT content is indicated for each set of measurements. (B) The dependence of  $I_B$  on AT content for non-urea and 3.5 M urea buffers (open blue and solid red symbols, respectively). The mean  $I_B$  values were determined by Gaussian fits to the  $I_B$  distributions. (C) The dependence of the mean translocation time as a function of AT content measured in either non-urea or 3.5 M urea buffers (open blue and solid red symbols, respectively).

where  $\bar{I}_B$  explicitly denotes the fact that we measure the *mean* blocked current (as opposed to the instantaneous blocked current level) of a collection of translocation events. Correspondingly,  $\bar{a}$  is a mean molecular cross-section, and  $d$  represents the pore diameter. Equation (1) can be reorganized in terms of the measured and unknown quantities in the experiment, namely  $\bar{a} = d\sqrt{1 - \bar{I}_B}$  where  $1 - \bar{I}_B$  is sometimes called the normalized event deficit [29]. Notably, when experiments are performed using the same nanopore size and under different conditions that may affect the mean cross-section of DNA (such as water and urea), it is constructive to extract the relative change in molecular cross-section, by using the diameter ratio,  $\xi$ , between the two experimental conditions:

$$\xi = \frac{\bar{a}_U}{\bar{a}_W} = \sqrt{\frac{1 - \bar{I}_B^U}{1 - \bar{I}_B^W}} \quad (2)$$

where U and W subscripts refer to urea or water buffers, respectively. The main advantage of equation (2) is that it removes the requirement to accurately measure the pore diameter, as long as the reference and the sample measurements are performed using the *same* nanopore.

Our results, presented in figure 3, qualitatively suggested that urea induces local, thermal fluctuations in the DNA helix,

which in turn induce a lower blocking current attributable to a slightly larger mean effective molecular cross-section  $\bar{a}_U$  in the presence of urea. To gain a better insight into the effects of urea-induced DNA thermal fluctuations on  $\bar{I}_B$ , we studied the dependence of the diameter ratio  $\xi$  on the urea concentration in our buffer (figure 4). In these experiments we used two different 800 bp dsDNA molecules with either 45% or 73% AT content, shown in solid squares or circles, respectively (see also gel image of sample molecules in figure SI-2 available at [stacks.iop.org/JPhysCM/22/454111/mmedia](http://stacks.iop.org/JPhysCM/22/454111/mmedia)). Each data point in this figure was obtained by acquiring at least 2000 individual events in both the reference and sample buffers to ensure sufficient statistics. The  $\bar{I}_B$  values and their errors (STD) were determined by fitting Gaussian functions to the blocked current distributions. The averaged  $I_B$  value for each translocation event represents a weighted sum of the partially blocked ion current arising from the fraction  $x_m$  of denatured base pairs within each DNA molecule. Comparing the two DNA molecules we observe in both cases a transition from  $\xi = 1$  at low urea concentrations to  $\xi \approx 1.3$  at 45% urea. The transition between these limits can be well described using a sigmoid function:

$$\xi = 1 + \frac{\xi_{\max} - 1}{1 + e^{-(C_{\text{urea}} - C_{1/2})/\text{rate}}} \quad (3)$$

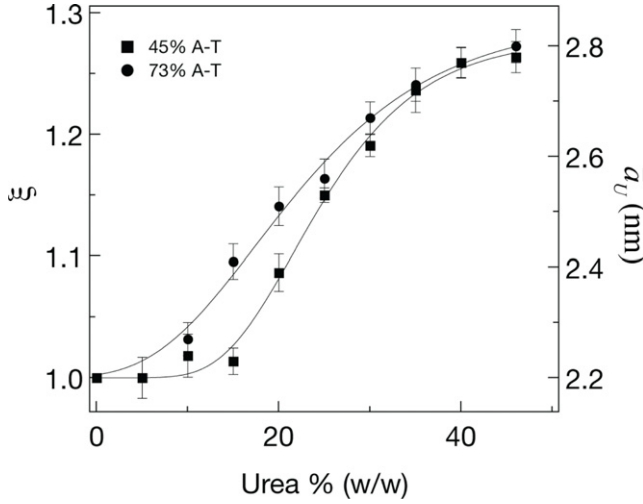


**Figure 4.** The dependence of the effective diameter ratio  $\xi$  on urea concentration measured using 800 bp DNA molecules having two different AT contents, as indicated. Solid lines represent fits to sigmoid functions (see the text). Using the known hydrodynamic diameter of dsDNA in non-urea buffer, the right axis represents the effective diameter of the DNA in urea buffer. We observe an increase of  $\sim 0.6$  nm in the mean diameter when changing from the non-urea buffer to 45% urea.

shown as a solid line in figure 4. As expected,  $C_{1/2}$ , the transition midpoint ( $\xi \approx 1.15$ ) of the 73% AT-content sample, is shifted towards lower urea concentration as compared to the sample with 45% AT content ( $20.9 \pm 1.1\%$  and  $24.4 \pm 0.8\%$ , respectively). These results are in contrast with those of control measurements performed with the same 3.3 nm pore under non-urea conditions (water), showing that, within experimental error, the fractional blockade levels and typical dwell-times were identical for both 800 bp DNA molecules:  $\bar{I}_B = 0.52 \pm 0.06$ ,  $t_D = 167 \pm 17 \mu s$  and  $\bar{I}_B = 0.53 \pm 0.05$ ,  $t_D = 156 \pm 7 \mu s$  for the 45% and the 73% AT-content DNA molecules, respectively. These results are in excellent agreement with our previous studies with the short,  $\sim 150$  bp long DNA molecules.

Previous dsDNA translocation studies with variable pore sizes indicated that the effective dsDNA cross-section can be very well approximated by its hydrodynamic value under water saline buffer, namely  $\bar{a}_W = 2.2$  nm [18]. It is therefore possible to use equation (2) to obtain an estimate of the weighted average dsDNA diameter at different urea concentrations, or  $\bar{a}_U = \xi \bar{a}_W$  for each value of the urea concentration  $C_{urea}$ . We find that for both molecules the *mean* effective diameter of the molecule increases by approximately 0.6 nm with increasing urea concentrations (figure 4, right axis).

Focusing on the DNA translocation dynamics, we characterized each of the DNA samples by fitting exponential functions to the distribution of dwell-times to obtain the typical timescale,  $\tau_D$ , in the presence of water or urea. As before, we are mainly interested in changes in the DNA dynamics induced by the presence of urea. We therefore calculate the ratio  $\tau_D^U/\tau_D^W$  at each urea concentration, measured for the two different DNA molecules, and plot the ratio as a function of urea concentration (figure 5, solid squares and circles for the 45% and 73% AT-

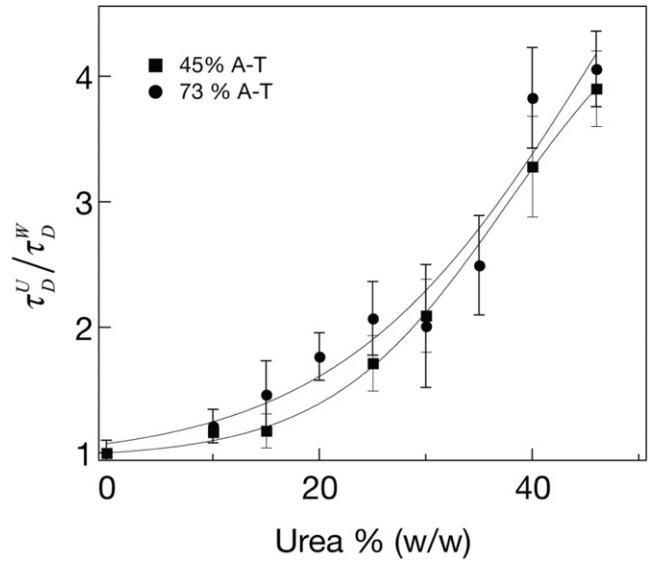


**Figure 5.** The dependence of the relative dwell-time (dwell-time measured in urea divided by the dwell-time measured in non-urea buffer using the same nanopore) on the urea concentration, measured for 800 bp DNA molecules with two different AT contents, as indicated. Solid lines are guides to the eye. The increase observed in the dwell-time is far beyond the expected increase based on buffer viscosity alone.

content DNA, respectively). We note two important features. First, for both DNA samples we observe a  $\sim 4$ -fold increase in the translocation time, when the urea concentration is increased from 0% to 45%. This is a much larger relative change than the less than twofold increase in the solution's viscosity over the same range of urea concentration. Second, unlike the clear distinction between the two samples observed in figure 4, the larger error bars in the translocation dynamics prohibit us from a clear distinction between the two DNA samples.

#### 4. Discussion and conclusions

We demonstrate for the first time that it is possible to detect local denaturation in dsDNA using solid-state nanopores. Solid-state nanopores in the 3–5 nm range offer the distinct advantage over larger nanopores in that they constrict the passage of dsDNA through the pore to one that is solely linear in fashion. We find that, at room temperature under high electrolyte strength conditions, the nanopore is unable to detect differences in the DNA structure given the low probability and lifetime of open DNA states [22, 23, 30–32]. However, by using urea as a well known denaturant we are able to gradually increase the probability of open region formation and, possibly, their size since the increase of urea concentrations lowers the DNA melting temperature. This increase in the DNA opening probability manifests itself in an increase in the mean effective molecular cross-section, of only a few Ångströms. Using the solid-state nanopores, we can detect this increase by comparing the partially blocked ion current during translocation events measured in urea to translocation events in a non-urea reference buffer.

Moreover, the increased effective molecular cross-section also manifests itself in an increased DNA translocation time, in a manner which is far greater than that of simple hydrodynamic effects. Additionally, a gradual increase in the DNA's AT content (keeping the same total DNA length constant) is correlated with both lower average blocked current levels and longer translocation times. These results are in line with previous studies indicating, on the basis of theory and experiment, an increased size and likelihood of DNA open regions in AT-rich DNA fragments given that A–T base pairs are weaker than G–C base pairs [22, 32–34].

One of the advantages of using solid-state nanopores for this study is their remarkable robustness to high concentrations of urea. Our results show that SiN-based pores display no discernible changes in pore geometry/charge at high urea concentrations, yielding a perfectly symmetrical current/voltage characteristic that can be explained by the changes in ion mobility due to increased viscosity. By contrast, DNA translocation dynamics is strongly affected by the presence of urea, in a manner that cannot be attributed to viscosity changes only. Moreover, the minor change in the dielectric constant of the urea solution as compared to the water buffer (<100 versus 80 at room temperature [35]) results in only a minor change in the net electrophoretic force applied on the biopolymer, and thus cannot account for the observed fourfold increase in translocation times (see figure 5). Rather, the retardation of DNA translocation at increasing urea concentration is attributed to the larger effective cross-section of the partially denatured regions in the molecule.

We have shown that dsDNA molecules, which are nearly identical in length and only differ in AT content, can be statistically discriminated with the use of urea. In non-urea solutions, the nanopore was unable to detect differences in the DNA structure. In urea solutions, we see that the relative blockade level increases as the AT content increases. We also find that the dwell-time increases in molecules with higher AT content, by a factor of  $\sim 2.5$ . By varying the urea concentrations, we studied the effects of urea on two 800 bp long DNA molecules, which differed only in AT content. We find that the *mean* hydrodynamic diameter of the molecules increases from 2.2 nm by about 0.6 nm in both cases, following a sigmoid function. Deciphering the exact nature of this functional behavior, which appears indicative of a cooperative mechanism of DNA local denaturation, is beyond the scope of this current study.

In addition to the increase in blockade levels, we observe a remarkable increase in the relative dwell-time with an increase in urea concentrations. As the physics governing the translocation process are currently poorly understood, elucidating the exact rationale behind this increase remains a focus of future studies. While a number of factors can affect translocation time, such as viscosity and interactions with pore walls [18], here we focus on the increase in the mean hydrodynamic diameter of the DNA helix, which is expected to result in increased friction with the pore and a retardation of the translocation process. We note, however, that other effects, such as local bends in the partially denatured dsDNA, might play a similar role of slowing down the translocation

process. Construction of a robust theoretical model that takes into account these possibilities is required to elucidate their relative importance.

In conclusion, the focus of our study is to establish that solid-state nanopores can be used as a new method for probing internal DNA structures. By using urea, which does not affect the nanopore's properties, we are able to detect thermal fluctuations in the DNA double helix structure. We have shown that the mean hydrodynamic diameter of DNA increases by  $\sim 0.6$  nm, exemplifying the excellent sensitivity of these small nanopores. Moreover, through further studies with additional osmolytes, we can gain further insight into the mechanism which governs the translocation process, by appreciating changes in blockade levels and dwell-times. The importance of our study on the effects of urea on DNA is twofold. First, we have established that solid-state nanopores can be used as a tool for high-resolution analysis of unlabeled DNA structural alterations. Furthermore, given the ability of the nanopore to analyze minute sample quantities, the total sample size is reduced by orders of magnitude when compared with traditional bulk methods such as CD or nuclear magnetic resonance. Second, through the inherent stability/robustness of solid-state materials to numerous solvents, we can employ a wide range of studies, which aim at further elucidating the physics which come into play when observing the passage of a charged polymer through nanoscale apertures.

## Acknowledgments

AM acknowledges financial support from NIH award number HG-004128.

## References

- [1] Healy K 2007 Nanopore-based single-molecule DNA analysis *Nanomedicine* **2** 459–81
- [2] Branton D, Deamer D W, Marziali A, Bayley H, Benner S A, Butler T, Di Ventra M, Garaj S, Hibbs A, Huang X, Jovanovich S B, Krstic P S, Lindsay S, Ling X S, Mastrangelo C H, Meller A, Oliver J S, Pershin Y V, Ramsey J M, Riehn R, Soni G V, Tabard-Cossa V, Wanunu M, Wiggins M and Schloss J A 2008 The potential and challenges of nanopore sequencing *Nat. Biotechnol.* **26** 1146–53
- [3] Howorka S and Siwy Z 2009 Nanopore analytics: sensing of single molecules *Chem. Soc. Rev.* **38** 2360–84
- [4] Wanunu M and Meller A 2008 Single-molecule analysis of nucleic acids and DNA–protein interactions using nanopores *Single-Molecule Techniques: A Laboratory Manual* ed P Selvin and T J Ha (Cold Spring Harbor, NY: Cold Spring Harbor Laboratory Press) pp 395–420
- [5] Dekker C 2007 Solid-state nanopores *Nat. Nanotechnol.* **2** 209–15
- [6] Marshall Don G 2003 The Coulter principle: foundation of an industry *JALA* **8** 72–81
- [7] Coulter W H 1953 Means of counting particles suspended in a fluid *USPTO* No. 2656508 USA
- [8] Storm A J, Chen J H, Ling X S, Zandbergen H W and Dekker C 2003 Fabrication of solid-state nanopores with single-nanometre precision *Nat. Mater.* **2** 537–40
- [9] Li J, Stein D, McMullan C, Branton D, Aziz M J and Golovchenko J A 2001 Ion-beam sculpting at nanometre length scales *Nature* **412** 166–9



- [10] Kim M J, Wanunu M, Bell D C and Meller A 2006 Rapid fabrication of uniformly sized nanopores and nanopore arrays for parallel DNA analysis *Adv. Mater.* **18** 3149–53
- [11] Venkatesan B M, Shah A B, Zuo J-M and Bashir R 2010 DNA sensing using nanocrystalline surface-enhanced Al<sub>2</sub>O<sub>3</sub> nanopore sensors *Adv. Funct. Mater.* **20** 1266–75
- [12] Wanunu M, Morrison W, Rabin Y, Grosberg A Y and Meller A 2010 Electrostatic focusing of unlabelled DNA into nanoscale pores using a salt gradient *Nat. Nanotechnol.* **5** 160–5
- [13] Gershow M and Golovchenko J A 2007 Recapturing and trapping single molecules with a solid-state nanopore *Nat. Nanotechnol.* **2** 775–9
- [14] Fologea D, Brandin E, Uplinger J, Branton D and Li J 2007 DNA conformation and base number simultaneously determined in a nanopore *Electrophoresis* **28** 3186–92
- [15] Singer A, Wanunu M, Morrison W, Kuhn H, Frank-Kamenetskii M and Meller A 2010 Nanopore based sequence specific detection of duplex DNA for genomic profiling *Nano Lett.* **10** 738–42
- [16] Soni G V and Meller A 2007 Progress toward ultrafast DNA sequencing using solid-state nanopores *Clin. Chem.* **53** 1996–2001
- [17] Wanunu M, Sutin J and Meller A 2009 DNA profiling using solid-state nanopores: detection of DNA-binding molecules *Nano Lett.* **9** 3498–502
- [18] Wanunu M, Sutin J, McNally B, Chow A and Meller A 2008 DNA translocation governed by interactions with solid-state nanopores *Biophys. J.* **95** 4716–25
- [19] Storm A J, Chen J H, Zandbergen H W and Dekker C 2005 Translocation of double-strand DNA through a silicon oxide nanopore *Phys. Rev. E* **71** 051903
- [20] McNally B, Wanunu M and Meller A 2008 Electromechanical unzipping of individual DNA molecules using synthetic sub-2 nm pores *Nano Lett.* **8** 3418–22
- [21] Vorlickova M and Palecek E 1970 Conformational changes in the region of the ends of the DNA molecule at premelting temperatures *FEBS Lett.* **7** 38–40
- [22] Frank-Kamenetskii M D and Lazurkin Y S 1974 Conformational changes in DNA molecules *Annu. Rev. Biophys. Bioeng.* **3** 127–50
- [23] Frank-Kamenetskii M D 1987 DNA chemistry—how the double helix breathes *Nature* **328** 17–8
- [24] Gueron M, Kochoyan M and Leroy J-L 1987 A single mode of DNA base-pair opening drives imino proton exchange *Nature* **328** 89–92
- [25] Fologea D, Uplinger J, Thomas B, McNabb D S and Li J 2005 Slowing DNA translocation in a solid-state nanopore *Nano Lett.* **5** 1734–7
- [26] Spink C H, Garbett N and Chaires J B 2007 Enthalpies of DNA melting in the presence of osmolytes *Biophys. Chem.* **126** 176–85
- [27] Gray D M, Ratliff R L and Vaughan M R 1992 Circular-dichroism spectroscopy of DNA *Methods Enzymol.* **211** 389–406
- [28] Aslanyan V M and Babayan Y S 1979 Effect of urea on the conformation of the double DNA helix *Biofizika* **24** 935–6
- [29] Fologea D, Gershow M, Ledden B, McNabb D S, Golovchenko J A and Li J 2005 Detecting single stranded DNA with a solid state nanopore *Nano Lett.* **5** 1905–9
- [30] Gueron M and Leroy J L 1995 Studies of base pair kinetics by NMR measurement of proton exchange *Methods Enzymol.* **261** 383–413
- [31] Frank-Kamenetskii M D 1985 Fluctuational motility of DNA *Nucleic Acids and Proteins* ed E Clementi (New York: Adenine Press) pp 417–32
- [32] Krueger A, Protozanova E and Frank-Kamenetskii M D 2006 Sequence-dependent base pair opening in DNA double helix *Biophys. J.* **90** 3091–9
- [33] Lukashin A V, Vologodskii A V, Frank-Kamenetskii M D and Lyubchenko Y L 1976 Fluctuational opening of double helix as revealed by theoretical and experimental study of DNA interaction with formaldehyde *J. Mol. Biol.* **108** 665–82
- [34] Yakovchuk P, Protozanova E and Frank-Kamenetskii M D 2006 Base-stacking and base-pairing contributions into thermal stability of the DNA double helix *Nucleic Acids Res.* **34** 564–74
- [35] Wyman J 1933 Dielectric constants: ethanol–diethyl ether and urea–water solutions between 0 and 50 °C *J. Am. Chem. Soc.* **55** 4116–21